Online extremum seeking-based optimized energy management strategy for hybrid electric tram considering fuel cell degradation

Qi Li, Tianhong Wang, Shihan Li, Weirong Chen, Hong Liu, Elena Virginia Breaz, Fei Gao

Online Extremum Seeking-Based Optimized Energy Management Strategy for Hybrid Electric Tram Considering Fuel Cell Degradation

Qi Li[a], Tianhong Wang[a, b*], Shihan Li[a], Weirong Chen[a], Hong Liu[c, d], Elena Breaz[b, e], Fei Gao[b]

[a] School of Electrical Engineering, Southwest Jiaotong University, Chengdu 610031, Sichuan Province, China

[b] FEMTO-ST Institute (UMR CNRS 6174), Energy Department, Univ. Bourgogne Franche-Comte, UTBM Rue Thierry Mieg, F-90010 Belfort Cedex, France

[c] Energy Research Institute, National Development and Reform Commission, Beijing 100038, PR China

[d] Academy of Macroeconomic Research, National Development and Reform Commission, Beijing 100038, PR China

[e] Technical University of Cluj-Napoca, Cluj-Napoca 400604, Romania

Abstract

In order to realize optimal power distribution between proton exchange membrane fuel cell and supercapacitor in hybrid electric tram, an online extremum seeking-based optimized energy management strategy is proposed in this work. Considering that the fuel cell is a complex nonlinear system, its performance will vary as the external parameters change, so it is necessary to consider the performance state of stack. An online extremum seeking algorithm is investigated in this work to seek the maximum power and maximum efficiency points by searching the variation in fuel cell

* Corresponding author.
E-mail address: bk20121444@my.swjtu.edu.cn (Tianhong Wang).

performance. Besides, this work also updates its "safe operating zone" based on the results of the online extremum seeking. This process is achieved by the adaptive recursive least square algorithm. Furthermore, in order to limit the power dynamic of fuel cell, the degradation of the stack is considered in this study. To guarantee the stable and continued operation of the electric tram, the state of charge fluctuation range of supercapacitor is also limited. The effectiveness of the presented method is successfully verified under scaled-down operating condition of hybrid electric tram on the reduced-scale test platform. The proposed method is also compared with state machine control and equivalent consumption minimization strategy to further demonstrate that it has advantages in hydrogen consumption, state of charge fluctuation, efficiency, and fuel cell output power dynamics.

Keywords: Proton exchange membrane fuel cell; Supercapacitor; System efficiency; Hydrogen consumption.

ABBREVIATIONS

PEMFC	Proton exchange membrane fuel cell	**FC**	Fuel cell
EMS	Energy management strategy	**MP**	Maximum power
LF-LRV	Low floor light rail vehicle	**ME**	Maximum efficiency
OBC	Optimization-based control	**RBC**	Rule-based control
SISO	Single-input single-output	**SMC**	State machine control
ESS	Energy storage system	**DP**	Dynamic programming
ECMS	Equivalent consumption minimization strategy	**SC**	Supercapacitor
ARLS	Adaptive recursive least square	**SOC**	State of charge
OES-EMS	Online extremum seeking-based optimized EMS		

1. Introduction

For the last years, as more and more countries attach importance to the energy crisis and environmental pollution [1], the research on proton exchange membrane fuel cell (PEMFC) has aroused considerable interest from scholars [2]. PEMFC, as a clean and renewable energy source, has been intensively developed in transportation such as automotive, rail transit and aerospace [3]. Because it has advantages of nearly zero-emission, high energy density, and quick start-up [4]. Nevertheless, the fuel cells (FC) have unavoidable shortcomings [5], such as slow electrochemical reaction, which makes it impossible to quickly track load dynamic response [6]. Therefore, the use of a single FC as a power supply in the power system, can not satisfy the load power demand [7]. PEMFCs are generally used in conjunction with another energy supply forming a hybrid system to meet power demand [8]. Supercapacitor (SC) has the advantages of quick response ability, high power density, and long cycle life. Therefore, PEMFC/SC hybrid system is often used to power electric trams [1], [3], [9].

Since the energy is allocated according to their special characteristics between two power sources (SC and FC) in the hybrid electric tram, and the FC can be employed in specific working modes [such as maximum power (MP) or maximum efficiency (ME)],

thus the energy management strategies (EMSs) are demanded. In addition, EMSs are expected to extend system's lifetime or improve system efficiency, so the EMSs play a pivotal role in hybrid electric tram and are generally divided into two main categories [10], [11]. They are optimization-based control (OBC) strategies and rule-based control (RBC) strategies.

The RBC is based on the operating characteristics of each power source, including state machine control (SMC), load following strategy, proportional integral derivative control [12], fuzzy logical control [13], and wavelet transform control [14]. These RBC strategies rely on a set of predefined rules based on the designer's engineering experience to determine the behavior of each power source at each sample time [15]. These strategies have the advantages of high reliability, easy implementation, and strong robustness. However, because the predefined rules based cannot be adjusted online in practical applications, it may result in poor performance in some systems [16]. The OBC is generally based on an objective function optimization. In addition, this kind of strategy usually defines the criterion of power change rate, fuel consumption, or system efficiency [17]. It mainly includes global optimization algorithms such as dynamic programming (DP), and instantaneous optimization algorithms such as equivalent consumption minimization strategy (ECMS) [18]. In order to optimize the operation of the hybrid system, Ali et al. [19] use the DP algorithm to optimize the EMS. This kind of strategy needs to know the global operation conditions in advance, and has a large amount of calculation, which is not suitable for on-line operation [15]. Zhang et al. [10] and Li et al. [20] both adopt PEMFC/battery/SC as powertrain to power a hybrid tramway, and in order to optimize system hydrogen consumption, ECMS is used to manage the output of each power source. Although these OBC strategies can achieve

good results in terms of hydrogen consumption or system efficiency, most of the work neglects the impact of stack degradation degree on hybrid systems.

Furthermore, as a complex nonlinear system, the performance of the PEMFC will change with the operating conditions such as temperature, gas humidity, and pressure [21], [22]. Unfortunately, most of the existing strategies ignore the impact of these factors on FC and treat FC as a constant model [17]. Obviously, when the FC operating parameters change, its output polarization curve will also change [23]. In addition, based on the research of [24] there is a "safe operating zone" during operation of the FC, and controlling the FC to operate in this zone is beneficial to improve the operating performance of FC. However, according to the above description, the "safe operating zone" of FC is movable. Therefore, in order to ameliorate the performance of the EMSs, it is necessary to identify the output curve of the FC.

Adaptive recursive least square (ARLS) algorithm is a data-driven online identification method that is often used to estimate system parameters [25]. This algorithm can be used to identify the PEMFC performance variations to improve the stack output voltage [26]. Based on the ARLS algorithm, our previous research proposes a forgetting factor recursive least square algorithm to search for the extreme point of PEMFC to improve system efficiency [27]. Moreover, the use of PEMFC at large scale is hindered by its cost and lifetime. If the cost could be partially solved by mass production, big efforts still need to be done regarding the lifetime. A well know factor which affects the FC lifetime is the output power fluctuation [4]. In order to extend the lifetime of PEMFC, the output power fluctuation should be limited. Therefore, its degradation degree should also be considered in the EMSs [28], [29]. At present, several EMSs for studying the degradation of PEMFC have been reported. The

unscented Kalman filter method is used in [30] to seek a variation in the stack performance. In addition, in order to adaptively allocate power according to the degradation degree of each stack, Kalman filter is used to estimate the stacks' operating parameters [31]. Moreover, the degradation model is considered in [32] to improve the operation performance of the stack. Although they can achieve a good result, they cannot further improve the durability of the PEMFC. In order to reflect the degradation degree of the stack in real-time, our previous study provides support for evaluating the degradation index of the stack in this study [33].

To summarize, there are many strategies to allocate the power between different power sources in hybrid system and research schemes to seek the optimal PEMFC performance. Nevertheless, it should be noted that few EMSs consider that the electrical performance of stack varies with operation parameters. Similarly, these strategies rarely link the energy allocation in a hybrid system and extremum tracking algorithm on PEMFC. In addition, although some references have studied the ME point seeking methods in the hybrid system, the SOC fluctuation is not considered [34]. Since the SC has the shortcoming of low energy density, in order to ensure that the hybrid electric tram can operate continuously and stably, the final state of charge (SOC) of the SC should be consistent with the initial SOC of the SC [35]. This study is based on our previous experimental results [27], which show that the identification algorithm for determining PEMFC degradation degree is applicable in real-time.

The main purpose of this study is to present an online extremum seeking-based optimized EMS (OES-EMS) for the hybrid electric tram. This strategy considers that the performance of the PEMFC will vary with the operating conditions, so an online extremum seeking is used to estimate the ME and MP operating points of the PEMFC.

The online extremum seeking process is implemented by the ARLS algorithm. Then, this work divides a "safe operating zone" for the PEMFC based on these two points. Moreover, this work also considers the performance state of FC and the SOC of SC to ameliorate the performance of the entire system. Furthermore, two PEMFCs with different degrees of degradation (One runs for about 10 hours and the other one runs for about 2500 hours) are adopted in this work. In order to test the performance of the presented OES-EMS in hybrid electric tram, a reduced-scale test platform powered by the PEMFC and SC is established. Then, the presented OES-EMS is applied to this experimental bench and demonstrated with a scaled-down operating condition of the hybrid electric tram. The key contributions of this study are summarized as follows:

1) Considering the variable output characteristics of the stack, an online extremum seeking method based on the ARLS algorithm is adopted.

2) In order to facilitate the adjustment of the output power of the stack according to its degradation degree, this work updates the PEMFC performance state online and divides a "safe operating zone" for the PEMFC with the ME point and the MP point as the boundary.

3) The electrical energy consumed by the SC is converted to the hydrogen energy consumed by the PEMFC, and the optimization problem of hydrogen consumption is converted to find the optimal reference power of the SC. In addition, in order to ameliorate the operating performance of SC and PEMFC, the SOC of SC and stack output power fluctuations are also adjusted in this study.

The remainder of this paper has the following structure. The configuration of the hybrid electric tram and the analysis of power sources are presented in Section 2; Section 3 elaborates the proposed energy management strategy; Experimental

verification and results analysis is performed in Section 4; Finally, the main conclusions and perspectives of this paper are discussed in Section 5.

2. Structure of the hybrid electric tram and description of the powertrain

2.1. Structure of the system

The 100% low floor light rail vehicle (LF-LRV) presented in this work is the world's first commercial PEMFC/SC hybrid electric tram and is jointly developed by Chinese manufacturer of Tangshan Railway Vehicle Co. Ltd and Clean Energy Lab of Southwest Jiaotong University in 2017. This hybrid electric tram and its architecture are depicted in Fig. 1. It includes two DC/DC converters, a SC, a PEMFC stack, some auxiliary systems, and a power distribution controller. The primary components and parameters of this tram are shown in TABLE I.

TABLE I. Primary components and parameters of hybrid electric tram.

Hybrid electric tram			
Tram weight	51.06t	Axle weight	10.5t
Max speed	30kM/h	Bus voltage	750V
Size (m^3)	30.19*2.65*3.5	Capacity	300 persons
PEMFC			
Manufacturer	Ballard (FCvelocityTM-HD6)	Type	Water-cooled
Rated power	150kW	Cell number	762
Voltage	530-710V	Max current	320A
Weight	305kg	Efficiency	55%
Hydrogen purity	99.999%	Hydrogen pressure	2.24Bar
Supercapacitor			
Manufacturer	Maxwell (BMOD0615)	Current	-300-700A
Voltage	200-528V	Capacity	45F
Weight	335kg	Set Numbers	11 series & 3 parallel

The FC is used as the main power supply to deliver the continuous and stable power demand for the hybrid electric tram. The SC is utilized as the secondary power source to provide fast peak power or recover the braking power for this tram [1], [3], [36]. In

addition, this hybrid electric tram also includes DC/AC converters, auxiliary systems, braking resistors, and so forth.

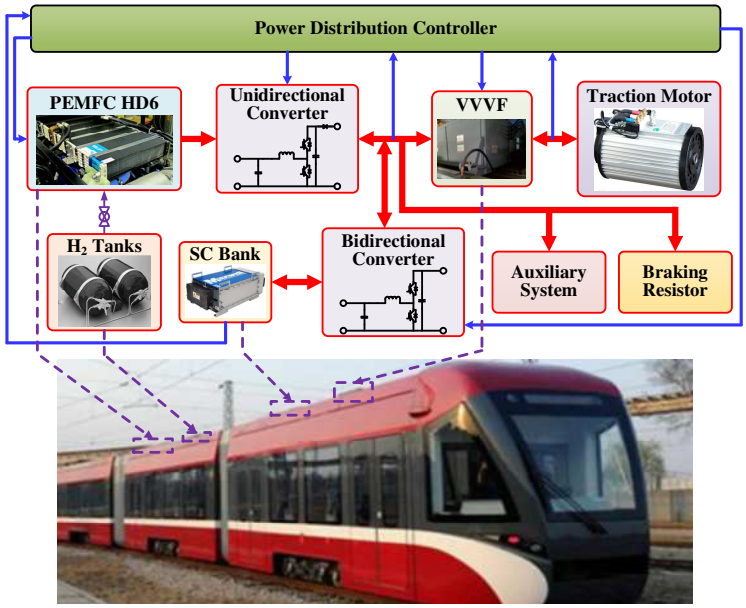

Fig. 1. The structure of PEMFC/SC hybrid electric tram and its components.

2.2. PEMFC and SC

The output polarization curves of HD6 FC stack used in LF-LRV is shown in Fig. 2. As it can be observed from Fig. 2 the functional relationship between the output voltage and the current of the stack can be expressed by the equation (1).

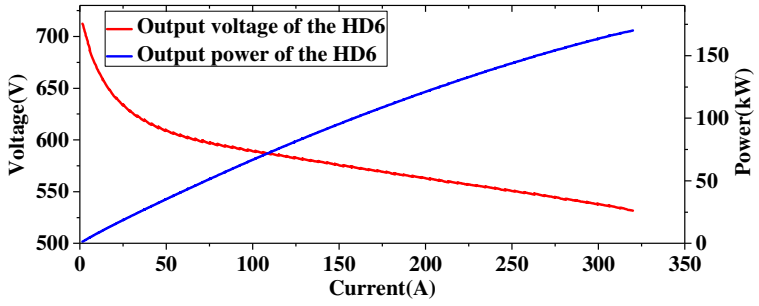

Fig. 2. Output characteristic curves of HD6.

$$V_{FC} = a_0 + a_1 I_{FC} + a_2 I_{FC}^2 \tag{1}$$

where I_{FC} represents the stack's real-time output current and V_{FC} denotes the output voltage of stack. In addition, according to the description in the Introduction section, the

coefficients (a_0, a_1, a_2) of equation (1) will change with the operation of the FC. Based on the research in [33] and [37], the output voltage and output power of stack can be used to evaluate stack's real-time degradation degree. Therefore, the degree of stack's degradation could be represented by [38]:

$$D_{FC} = \frac{V_{FC,Irated}}{V_{rated}} \tag{2}$$

where V_{rated} is the rated voltage of the selected stack and $V_{\text{FC,Irated}}$ is the voltage of stack when the stack outputs the rated current at the current degradation level. In addition, the $V_{\text{FC,Irated}}$ can be calculated through equation (1), and the parameters of equation (1) can be estimated by the ARLS algorithm. D_{FC} is a quantity that characterizes the degradation degree of stack.

To improve the performance of FC, the stack should work in the "safe operating zone" (bound by the stack's ME and the MP points) as much as possible [23], [24]. Besides, the FC system efficiency could be calculated by [21]:

$$\eta_{FCS} = \frac{V_{SFC} I_{FC}}{-\Delta H_{LHV} I_{FC} \times 2F} \times \left(1 - \frac{P_{aux}}{P_{FC}}\right) = \frac{V_{SFC}}{1.254}\left(1 - \frac{P_{aux}}{P_{FC}}\right). \tag{3}$$

In equation (3), V_{SFC} denotes the voltage of a single cell, F presents the Faraday constant, P_{FC} denotes the output power from the PEMFC stack, and P_{aux} presents the power used by auxiliary systems. In addition, this study uses the hydrogen lower heating value to calculate the efficiency, so the value of ΔH_{LHV} is 241.98kJ/mol.

As stated before, a SC is used as an energy storage system (ESS) to recover braking power or provide the rapidly changing power. The SOC of SC is a particularly important indicator for power distribution method, and this parameter can be calculated by the following equations [1]:

$$SOC(t+1) = SOC(t) + \Delta SOC(t) \tag{4}$$

with

$$\Delta SOC(t) = \frac{\int_{t-1}^{t} I_{SC} dt}{C_{SC} V_{SC,rate}} \tag{5}$$

where C_{SC}, I_{SC}, and $V_{SC,rate}$ present the SC capacity, output current of SC, and rated voltage of SC, respectively.

2.3. DC/DC converters

Power electronic equipment is required to implement power distribution in the hybrid electric tram. Therefore, the DC/DC converters are employed in this work to stabilize the voltage of DC bus and control the output power of the PEMFC and SC. The maximum voltage of the HD6 is 710V, which is lower than the bus reference voltage. Therefore, a DC/DC unidirectional boost converter is selected to connect the stack to the bus. In addition, the maximum voltage of the SC is 528V, which is also lower than the reference voltage of DC bus. Thus, a DC/DC bidirectional buck/boost converter is adopted.

3. Energy management strategies

To realize optimal power allocation between the SC and PEMFC, so that the hydrogen consumption can be reduced and the performance of PEMFC can be improved, this paper considers the factors such as PEMFC degradation degree and SOC of SC. In addition, considering that the operating performance of the PEMFC will change with the external conditions, the polarization curves should also be identified. Therefore, the main purpose of ARLS algorithm presented in this work is to estimate the boundary values of the “safe operating zone” and evaluate the current degradation

degree of PEMFC. Moreover, in order to highlight the superiority of the proposed strategy, the ECMS and the SMC strategy are used for comparative analysis.

3.1. Design of the proposed OES-EMS

3.1.1. Optimized energy management strategy

In order to realize the purpose of minimizing hydrogen consumption and being able to manage power allocation between PEMFC and SC in real-time, a power distribution strategy is developed with reference to the ECMS. The core step of the ECMS is to convert the electric energy consumption by the ESS into equivalent fuel consumption, and the main purpose of the ECMS is to reduce the hybrid system's total fuel consumption. The total instantaneous fuel consumption of the system (C_{sys}) can be defined as the sum of the indirect equivalent fuel consumption of SC (C_{SC}) and the direct hydrogen consumption of the PEMFC (C_{FC}). The instantaneous fuel consumption can be expressed by the following mathematical expression:

$$C_{sys}(t) = C_{FC}(t) + C_{SC}(t) = f_1\left(P_{FC}(t)\right) + f_2\left(P_{SC}(t)\right). \tag{6}$$

In equation (6), $P_{SC}(t)$ and $P_{FC}(t)$ are real-time output power of SC and PEMFC, respectively. The $f_1(P_{FC}(t))$ can be obtained by [11]:

$$f_1\left(P_{FC}(t)\right) = \frac{P_{FC}(t)}{\Delta H_{LHV}\eta_{FCS}(t)}. \tag{7}$$

In addition, the equivalent fuel consumption of SC can be calculated by the SOC of SC and output power of SC [1], thus, the $f_2(P_{SC}(t))$ can be calculated by:

$$f_2\left(P_{SC}(t)\right) = \begin{cases} \dfrac{P_{SC}(t)}{\Delta H_{LHV}\eta_{Bdc/dc}\eta_{FCS,avg}\eta_{dis}(t)\eta_{chg,avg}} & P_{SC}(t) \geq 0 \\ \dfrac{P_{SC}(t)\eta_{chg}(t)\eta_{dis,avg}}{\Delta H_{LHV}\eta_{Bdc/dc}\eta_{FCS,avg}} & P_{SC}(t) < 0 \end{cases}. \tag{8}$$

In this equation, $\eta_{FCS,avg}$ represents PEMFC average efficiency, $\eta_{dis,avg}$ and $\eta_{chg,avg}$ denote the average discharge and charge efficiency of SC, respectively, and $\eta_{Bdc/dc}$ represents the bidirectional converter efficiency. In addition, $\eta_{dis}(t)$ and $\eta_{chg}(t)$ represent the discharge and charge efficiency of SC, respectively. The efficiency of SC can be expressed by [3]:

$$\eta_{SC}(t)=\begin{cases}\eta_{dis}(t)=\dfrac{1}{2}\left(1+\sqrt{1-\dfrac{4R_{SC}P_{SC}(t)}{U_{OCV}^2}}\right)\\ \eta_{chg}(t)=2\Big/\left(1+\sqrt{1-\dfrac{4R_{SC}P_{SC}(t)}{U_{OCV}^2}}\right)\end{cases}. \tag{9}$$

where R_{SC} and U_{OCV} represent the internal resistance and output voltage of SC, respectively.

In order to keep PEMFC working as far as possible in the "safe operating zone" while ensuring that the end-state SOC of SC is close to the beginning state, two nonlinear constraints (K_{FC} and K_{SC}) are considered in the presented strategy. In addition, the degradation degree of PEMFC is also considered in this work, thus to reach optimal power distribution between SC and PEMFC, the optimization problem can be converted into a mathematical problem that solves the optimal solution of the following equation.

$$\min C_{sys}(t)=\min\left(f_1^*\left(P_{FC}(t)\right)+f_2^*\left(P_{SC}(t)\right)\right), \tag{10}$$

with

$$\begin{cases}f_1^*\left(P_{FC}(t)\right)=\dfrac{1}{D_{FC}}K_{FC}f_1\left(P_{FC}(t)\right)\\ f_2^*\left(P_{SC}(t)\right)=K_{SC}f_2\left(P_{SC}(t)\right)\end{cases}. \tag{11}$$

In addition, K_{FC} is the operating region constraint of PEMFC, and this penalty coefficient is used to keep the PEMFC operating as much as possible in its "safe

operating zone". The K_{SC} is used to constrain the variation between SC initial SOC and final SOC.

The PEMFC operating region constraint K_{FC} is described as:

$$K_{FC}=\begin{cases}\left(1+2\times\dfrac{\left|P_{FC}-P_{FC,MEP}\right|}{P_{FC,MPP}-P_{FC,MEP}}\right)^{2} & P_{FC,MEP}<P_{FC}<P_{FC,MPP}\\ \left(1+2\times\dfrac{\left|P_{FC}-P_{FC,MEP}\right|}{P_{FC,MPP}-P_{FC,MEP}}\right)^{4} & P_{FC}\le P_{FC,MEP}\end{cases} \tag{12}$$

where $P_{FC,MEP}$ denotes the ME operating point power of the PEMFC, $P_{FC,MPP}$ represents the MP operating point power of the PEMFC. According to our previous study [27], the ME and MP of the PEMFC will change with the working conditions. Therefore, an online extremum seeking algorithm is presented in this work to seek the ME and MP points of PEMFC.

The constraint of SC SOC KSC is defined as follows:

$$K_{SC}=\begin{cases}\left(1-2\times\dfrac{SOC(t)-SOC_{init}}{SOC_{\max}-SOC_{\min}}\right)^{2} & SOC_{\min}\le SOC(t)\le SOC_{\max}\\ \left(1-2\times\dfrac{SOC(t)-SOC_{init}}{SOC_{\max}-SOC_{\min}}\right)^{4} & \text{else}\end{cases}. \tag{13}$$

where $SOC_{\max}$, $SOC_{\min}$ are the upper and lower limits of the SC SOC (0.9 and 0.2), respectively. K_{SC} can make the SC final SOC close to its initial SOC. Taking into account that the SC has the disadvantage of low energy density, therefore, the SOC variation of the beginning state and end state of SC within a driving cycle should be as small as passible to guarantee that the hybrid electric tram can operate continuously and safely [35]. In addition, it should be mentioned that the longer the stack is working under transient load conditions, the more severe is the degradation degree and the shorter is the lifespan [38]. Thus, the output power fluctuations should be limited when

the degradation of PEMFC is severe. Therefore, the D_{FC} [obtained by ARLS algorithm and equation (2)] is used in this study for smoothing out the output power of the stack, to adjust PEMFC output power based on stack's real-time degradation degree.

In addition, some constraints should be added to the power sources.

$$\begin{cases} SOC_{\min} \le SOC(t) \le SOC_{\max} \\ P_{FC,\min} \le P_{FC} \le P_{FC,\max} \\ D_{FC}\Delta P_{FC,decrease} \le \dfrac{P_{FC}(t)}{dt} \le D_{FC}\Delta P_{FC,increase} \\ P_{SC,\min} \le P_{SC} \le P_{SC,\max} \end{cases} \tag{14}$$

where $P_{FC,max}$ and $P_{FC,min}$ represent the maximal and minimum power of stack, respectively. $P_{FC,decrease}$ and $P_{FC,increase}$ are used to limit the dynamic power fluctuations of PEMFC. $P_{SC,min}$ and $P_{SC,max}$ denote the maximal charge and discharge power of SC, respectively.

Then the PEMFC optimal reference power $P_{FC,opt}$ can be obtained.

$$P_{FC,opt} = P_{demand} - P_{SC,opt}. \tag{15}$$

In this equation, P_{demand} represents the load power and $P_{SC,opt}$ represents the optimal power of SC.

3.1.2. Online extremum seeking process based on ARLS algorithm

As can be seen from the above description, the online extremum seeking method plays a prominent role in the presented OES-EMS. This algorithm is proposed to estimate the parameters of equation (1) and seek the ME and MP operating points of PEMFC throughout the operating cycle. Then the degradation degree D_{FC} and the "safe operating zone" of the PEMFC can be determined. The ARLS algorithm is carefully described in our previous study, and its performance has been verified by experimental results [27].

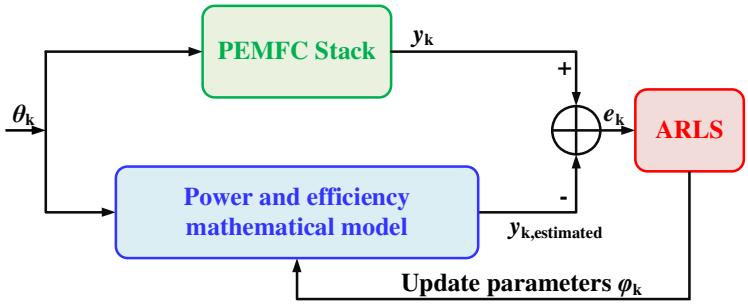

Fig. 3. Stack's parameters identification flowchart using the ARLS algorithm.

As shown in Fig. 3, the ARLS algorithm could be represented by a single-input single-output (SISO) model as follows:

$$[y(k)]=[\varphi(k)]^T[\theta(k)]+[e(k)]. \tag{16}$$

In equation (16), φ(k) denotes the regressor vector, θ(k) represents the system parameters, e(k) represents the stochastic noise and k denotes time step. The purpose of the ARLS algorithm is to minimize e(k). This process can be expressed as minimizing the following performance indicator.

$$J=\sum_{k=1}^{L}\beta^{L-k}e^2(k) \tag{17}$$

where β denotes the forgetting factor, which is employed to track the variation of the parameters during a time variation.

$$\begin{cases}\theta(k+1)=\theta(k)+K(k+1)\left[y(k+1)-\varphi^T(k+1)\theta(k)\right]\\ K(k+1)=\dfrac{P(k)\varphi(k+1)}{\beta+\varphi^T(k+1)P(k)\varphi(k+1)}\\ P(k+1)=\dfrac{1}{\beta}\left[I-K(k+1)\varphi^T(k+1)\right]P(k)\\ e(k+1)=y(k+1)-\varphi^T(k+1)\theta(k)\end{cases}. \tag{18}$$

In equation (18), P(k) denotes the covariance matrix of the identification error and K(k) represents the Kalman gain. Then, the presented ARLS algorithm can be implemented by the equation (18).

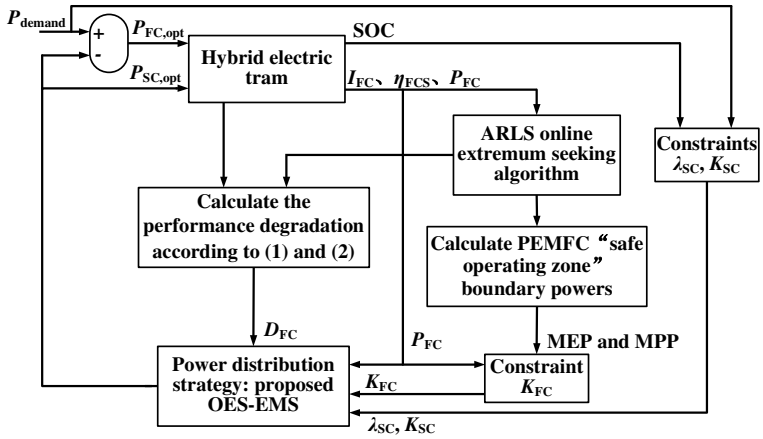

Fig. 4. The implementation process of the proposed OES-EMS.

As shown in Fig. 4, the specific implementation process of the proposed OES-EMS is as follows:

STEP1: Use the online identification method based on the ARLS algorithm shown in equation (19) to obtain the ME and MP points of the FC, thereby determining the "safe operating zone" of the stack;

STEP2: Calculate the current degradation degree of the FC according to identification results and equations (1) and (2);

STEP3: According to equations (13) and (14), solve the penalty coefficients for power sources operation;

STEP4: Use equations (6)-(11) to solve the real-time optimal output power of the SC, and then obtain the optimal output power of the PEMFC according to equation (15);

STEP5: Use the DC/DC converter cascaded with the PEMFC to control the stack output reference power.

Through above steps, the purpose of reaching optimal power distribution between PEMFC and SC can be realized.

3.2. Design of equivalent consumption minimization strategy

Based on [10], the equivalent consumption minimization strategy can be described as the following optimization problem.

$$P_{FC,opt} = \arg\min C_{sys} = \arg\min\left(C_{FC} + \lambda_{SC} C_{SC}\right). \tag{19}$$

The penalty factor λ_{SC} can be expressed by:

$$\lambda_{SC} = 1 - \frac{2\mu\left(SOC(t) - 0.5\left(SOC_{\max} + SOC_{\min}\right)\right)}{SOC_{\max} - SOC_{\min}} \tag{20}$$

where μ is used to adjust the λ_{SC} to adapt to different working conditions.

The power sources in the system should meet the following constraints.

$$\begin{cases} SOC_{\min} \le SOC \le SOC_{\max} \\ P_{FC,\min} \le P_{FC} \le P_{FC,\max} \\ P_{SC,\min} \le P_{SC} \le P_{SC,\max} \end{cases}. \tag{21}$$

The ECMS has the ability to ameliorate the total hydrogen consumption of system and is often used in the real-time applications [1].

3.3. Design of state machine control strategy

In addition to the ECMS, this work also uses a rule-based state machine control strategy as a benchmark to highlight the superiority of the proposed OES-EMS. According to the designer's experience and research of [12] and [39], the state machine control strategy designed in this work consists of six states, as shown in TABLE II.

TABLE II. State machine control strategy decisions.

SOC state	P_{demand}	State	$P_{FC,opt}$
If SOC low	$P_{demand} > P_{FC,max}$	1	$P_{FC,opt} = P_{FC,max}$
If SOC low	$P_{demand} \le P_{FC,max}$	2	$P_{FC,opt} = P_{FC,max} - P_{SC,min}$
If SOC normal	$P_{demand} \ge P_{FC,max}$	3	$P_{FC,opt} = P_{FC,max}$
If SOC normal	$P_{demand} \in [P_{FC,MEP}, P_{FC,max}]$	4	$P_{FC,opt} = P_{demand}$
If SOC normal	$P_{demand} < P_{FC,MEP}$	5	$P_{FC,opt} = P_{FC,MEP}$
If SOC high	-	6	$P_{FC,opt} = P_{FC,min}$

In TABLE II, the SOC of SC is divided into three areas: low (SOC<0.2), normal (0.2<SOC<0.9), and high (SOC>0.9). Through the TABLE II, the state machine control strategy can be realized.

4. Experimental and Results Analysis

The use of the tram directly to verify the strategy presented in this study is unsafe and uneconomical [40], therefore we build a reduced-scale experimental platform shown in Fig. 5. The reduced-scale experimental bench is established based on the structure of the LF-LRV, and is used to prove the superiority of the proposed OES-EMS. The key parameters of the power sources and the established DC/DC converters will be described in detail. In addition, the voltage and current sensors and signal conditioning unit are utilized to measure the voltage and current of all power supplies. These electrical signals are acquired and recorded by the NI-DAQ. Moreover, the ITECH's electrical load (IT-E502) and DC power supply (IT6522C) are used in this work to simulate the actual scaled-down hybrid electric tram drive cycle.

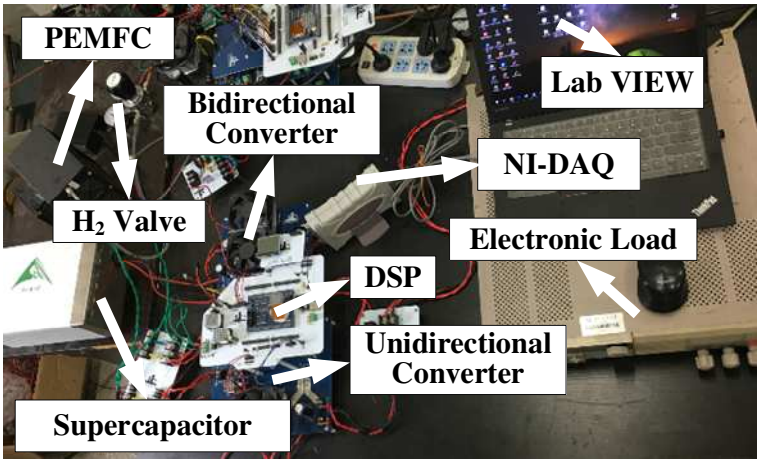

Fig. 5. The established reduced-scale experimental bench.

To better highlight the superiority of the presented OES-EMS, the optimization-based ECMS and rule-based state machine control strategy are also employed in this study. Furthermore, a degraded stack (S-1300 No.1) is used in this experiment to demonstrate

the effect of the constraint D_{FC}. The different strategies and constraints are listed in TABLE III.

TABLE III. Strategies and constraints for experiments.

Experiment	Strategy	Constraint	Stack state
1	SMC	-	Good-performing
2	ECMS	-	Good-performing
3	OES-EMS	K_{FC}, K_{SC}, D_{FC}	Good-performing
4	OES-EMS	K_{FC}, K_{SC}, D_{FC}	Aged
5	OES-EMS	K_{FC}, K_{SC}, D_{FC}=1	Aged

As shown in TABLE III, in order to verify the superiority and effect of the proposed OES-EMS, this study carries out the above five comparative experiments. Experiments 1-3 comparatively analyze the proposed OES-EMS, SMC strategy and ECMS. Besides, experiments 4 and 5 are used to analyze the effect of constraint D_{FC}.

4.1. Power sources and converters

To test and verify the effectiveness of the proposed OES-EMS, in addition to the SMC and ECMS, two PEMFC stacks with rated power of 1.3kW produced by Sunlait Company are also employed in this study. The models of these two stacks are S-1300 No.1 and S-1300 No.2, respectively. The S-1300 No.1 stack has a long operating time (about 2500 hours), so the degradation degree is obvious. The S-1300 No.2 stack has a shorter running time (about 10 hours), thus the performance of S-1300 No.2 stack is close to the ideal state. The polarization curves of these two stacks are shown in Fig. 6. In addition, the output voltage curve of FC can be expressed by equation (1).

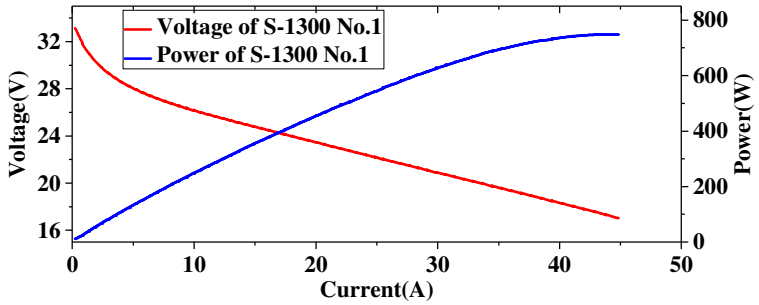

(a)

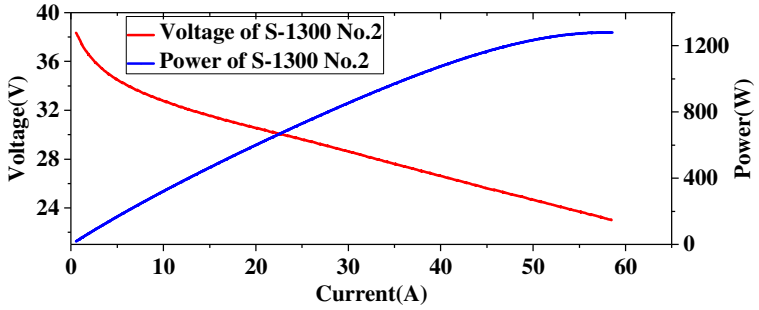

(b)

Fig. 6. Output characteristic curves of (a) S-1300 No.1 system, (b) S-1300 No.2 system.

According to equation (3), the efficiency curves of S-1300 No.1 and No.2 can be obtained, and the "safe operating zone" is shown in Fig. 7. From the previous description, it can be seen that this zone is movable. Therefore, this study uses the ARLS algorithm to estimate the ME point and MP point of the FC.

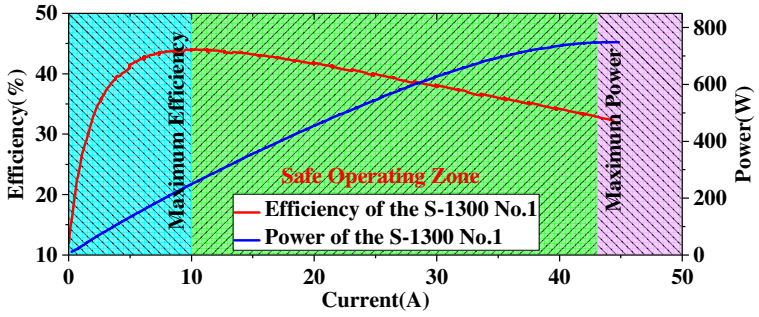

(a)

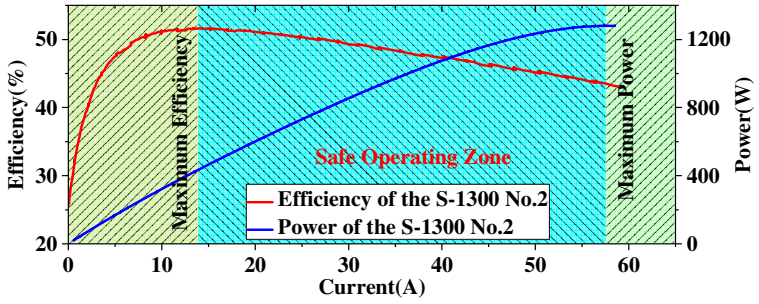

(b)

Fig. 7. Efficiency curves and the "safe operating zone" of (a) S-1300 No.1 system, (b) S-1300 No.2 system.

It can be seen from Fig. 7 that the efficiency of the underperforming PEMFC (S-1300 No.1) is lower than the ideal performance stack (S-1300 No.2). In addition, the maximum output power of stack No.2 is significantly higher than the maximum output power of stack No.1. Moreover, according to equation (7), the fuel consumption rate of the two selected PEMFCs can be obtained, as shown in Fig. 8. Furthermore, the primary parameters of S-1300 No.1, S-1300 No.2, and SC are listed in TABLE IV.

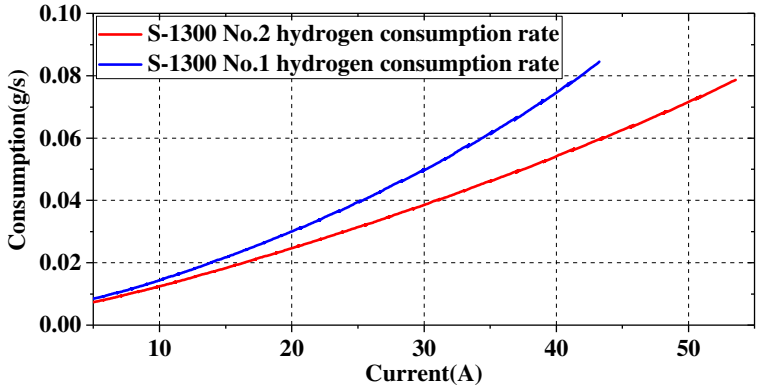

Fig. 8. Hydrogen consumption rate curves (g/s) of S-1300 No.1 and No.2 PEMFC systems.

TABLE IV. Main operating parameters of the stack and the SC.

FC(S-1300)			
Type	PEMFC	Output voltage	23-38V
Rated power	1300W	Max operating temperature	65℃
Max current	58.3A	Weight	6.7kg
SC			
Rated capacitance	58F	Rated voltage	32V
Specific power	6Wh/kg	Weight	4.3kg

To simplify the calculation and speed up the control, according to literature [41] and Fig. 8, the fuel consumption of the PEMFC can be expressed by the polynomial fitting function of P_{FC}, as shown in following:

$$f_1(P_{FC}) = \begin{cases} b_0 + b_1 P_{FC1} + b_2 P_{FC1}^2 \\ c_0 + c_1 P_{FC2} + c_2 P_{FC2}^2 \end{cases}. \tag{22}$$

In addition, based on the selected PEMFC and SC, this work adopts the NQ60W60 module produced by the Synqor Manufacturer to build two DC/DC converters, and the primary parameters of the established converters are listed in TABLE V.

TABLE V. Main power generation parameters of the established converters.

	Bidirectional converter	Unidirectional converter
Input side capacitor	60V/1000μF	60V/2200μF
Output side capacitor	60V/1500μF	60V/1500μF
Output voltage	32V or 48V	48V
Input voltage	<48V	<48V

4.2. Experimental tracking of the ME and MP points of PEMFC

In order to test the feasibility of the proposed online extremum seeking method, this section conducts a validation experiment using the testbench shown in Fig. 5. The test condition is shown in Fig. 9. What is more, it should be noted that since it is difficult to directly verify the performance of the identification algorithm, this work first uses the ARLS algorithm to identify the FC output curves, and then sets the ME and MP points as the reference power based on the identification results to indirectly demonstrate the effectiveness of the ARLS algorithm. This also means that in this validation experiment, the PEMFC always works at the ME point or MP point. The function of the SC in this experiment is only to maintain the system power balance, and the PEMFC uses S-1300 No.2. Fig. 10 shows the results of using the proposed ARLS algorithm to seek the ME and MP operating points.

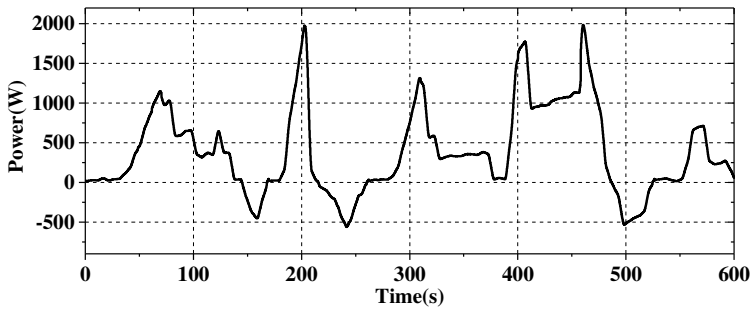

Fig. 9. Working condition for testing the ARLS algorithm.

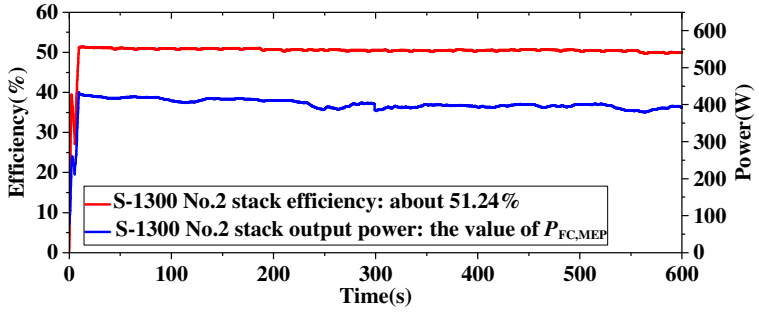

(a)

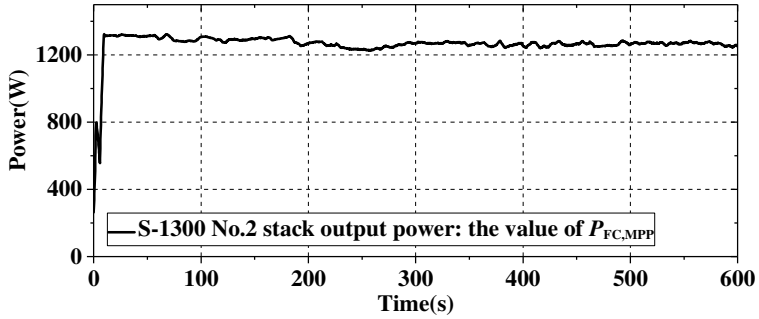

(b)

Fig. 10. The ARLS algorithm performance verification. (a) S-1300 No.2 stack ME operating point power. (b) S-1300 No.2 stack MP operating point power.

The results in Fig. 10 show that as the external operating parameters change, the ME and MP operating points of PEMFC will indeed fluctuate. Besides, the effectiveness of the online seeking method based on the ARLS algorithm is also verified.

4.3. Power allocation of PEMFC and SC using different EMSs and constraints

The scaled-down hybrid electric tram power demand is shown in Fig. 11, with power ranging from -750W to 2000W. In addition, the SC and PEMFC output power curves under the control of different EMSs are shown in Fig. 12. Specific indicators are analyzed in the next sections. It can be clearly observed that all the strategies can fulfill the load demand, and the PEMFC provides the main power of the hybrid system. Besides, the SC provides the required instantaneous power or recovers system braking and excess energy.

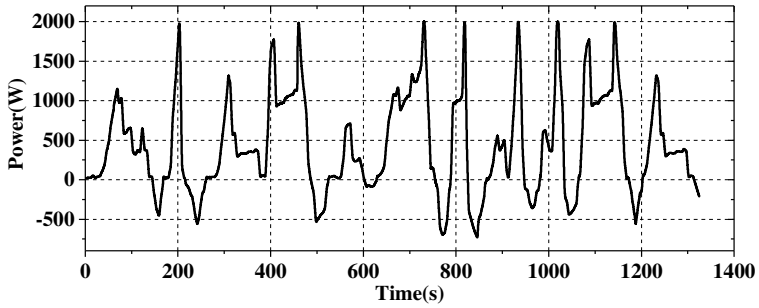

Fig. 11. Scaled-down power demand of the hybrid electric tram.

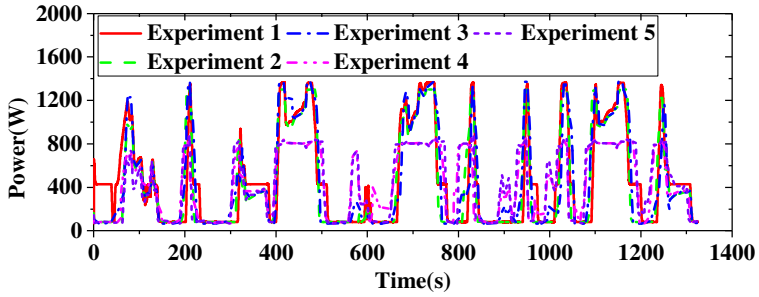

(a)

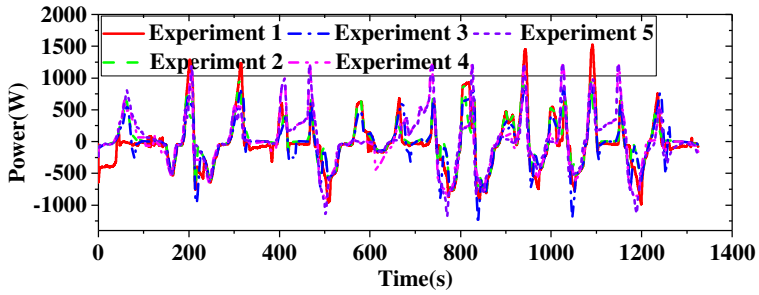

(b)

Fig. 12. Power distribution curves of different power sources in different experiments (a) PEMFC output power; (b) SC output power.

4.4. Comparative analysis of different strategies

Fig. 12 presents the power output curves of the PEMFC and SC when different EMSs (SMC strategy, ECMS and OES-EMS) and different constraints are used. To test the performance of the presented OES-EMS, the SOC fluctuation of SC, the efficiency of PEMFC, system hydrogen consumption, and power sources operating stress are analyzed in this section.

4.4.1. SOC comparative analysis

As the only ESS in the hybrid system, the SC plays a particularly important role. The SOC curves of SC under the control of different strategies are presented in Fig. 13. In order to facilitate the comparison of experimental results, the initial SC SOC values in all the strategies are set to the same value (about 74%). In this section, the current and voltage of the SC can be measured directly through the sensors, and the SOC of SC is calculated through equations (4) and (5).

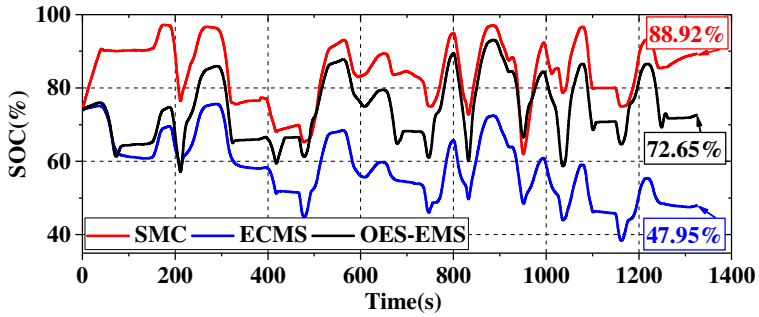

Fig. 13. The SOC curves of SC under the control of different strategies.

In Fig. 13, the end-state SC SOC of the presented OES-EMS, SMC strategy, and the ECMS are 72.65% (ΔSOC is about 2%), 88.92% (ΔSOC is about 15%), and 47.95% (ΔSOC is about 27%), respectively. Obviously, the presented strategy can ensure that the SC end-state SOC is close to its beginning state SOC. Compared with the ECMS and SMC strategy, the SOC of proposed OES-EMS has the smallest variation between the beginning state and end state, which helps to guarantee the stable and continuous operation of the hybrid electric tram [3].

4.4.2. Comparative analysis of the efficiency and hydrogen consumption

The efficiency of the PEMFC can be calculated by equation (3). Fig. 14 shows the efficiency curves of PEMFCs under the control of different strategies.. When using the proposed OES-EMS, the average efficiency of the PEMFC is 38.09%, which is 5.62% higher than that of the ECMS and is 0.97% higher than that of the SMC strategy. It can

be seen that the proposed OES-EMS can improve the operating efficiency of the PEMFC and improve the system economy.

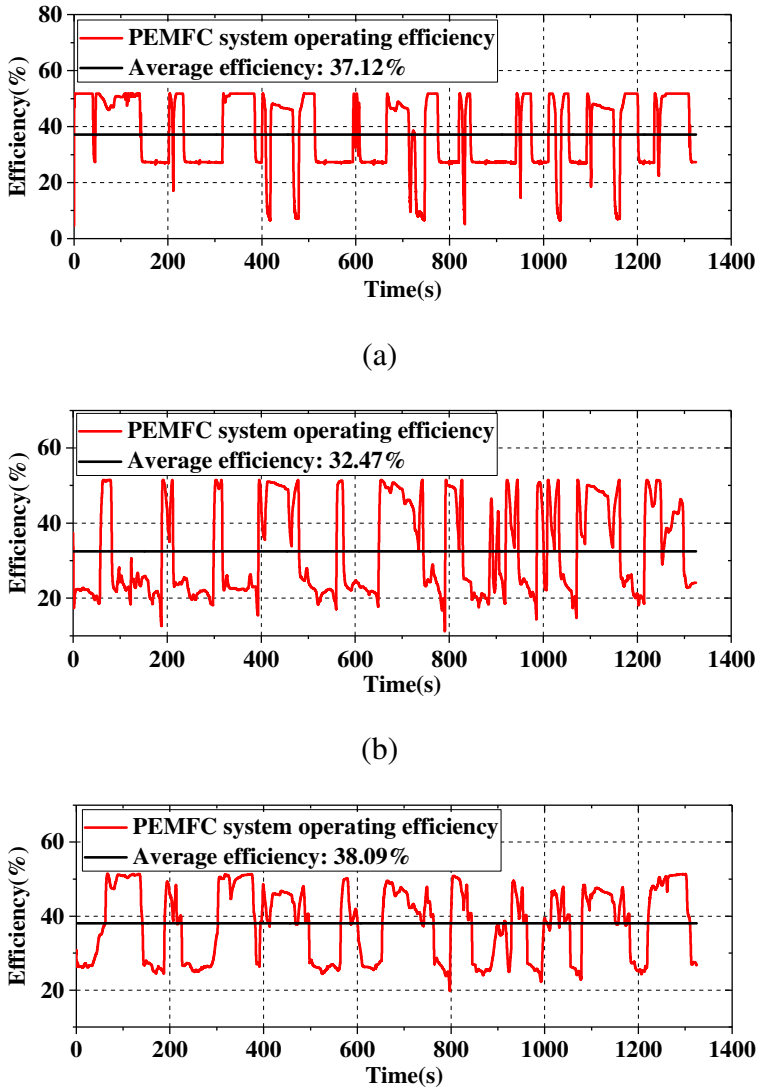

Fig. 14. PEMFC efficiency curves using different strategies. (a) SMC strategy; (b) ECMS; (c) OES-EMS.

Moreover, the fuel consumption rate of the PEMFC and SC could be obtained by equations (7) and (8). Then the total fuel consumption mass can be calculated by:

$$C_{H_2,total} = C_{H_2,FC} + C_{H_2,SC}, \tag{23}$$

with

$$\begin{cases} C_{H_2,FC} = \int_0^T C_{FC}(t)\,dt \\ C_{H_2,SC} = \int_0^T C_{SC}(t)\,dt \end{cases} \tag{24}$$

where $C_{H2,SC}$ and $C_{H2,FC}$ denote the equivalent fuel consumption of the SC and hydrogen consumption of PEMFC, respectively. By calculating the equivalent hydrogen consumption rate of the SC and the fuel consumption rate of the stack in real-time, the total amount of hydrogen consumption can be obtained, as shown in Fig. 13. The total mass of hydrogen consumed by the system using SMC strategy, ECMS, and OES-EMS is 32.47g, 23.8g, and 18.21g, respectively. It can be seen that in these strategies, the total hydrogen consumption of the presented OES-EMS is the smallest.

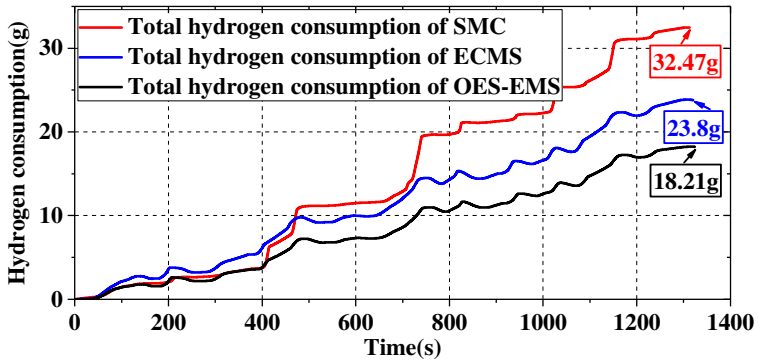

Fig. 15. Total hydrogen consumption curves using different strategies.

4.4.3. Comparative analysis of the power sources operating stress

According to [27] the key factor that affects the performance of power sources is related to power fluctuations. The operating stress analysis results of power sources using different strategies are presented in Fig. 16. These results are obtained using Haar wavelet transform technique, and the fluctuation distributions of PEMFC and SC provide a clear indication of how often each power source is solicited.

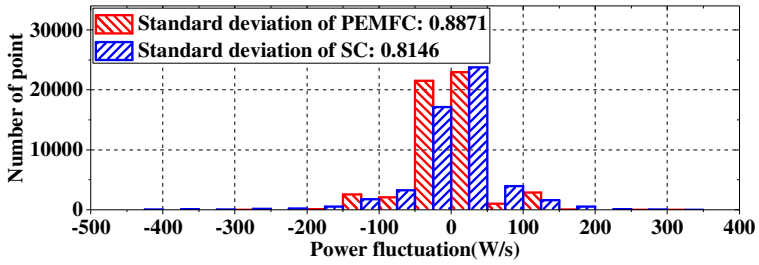

(a)

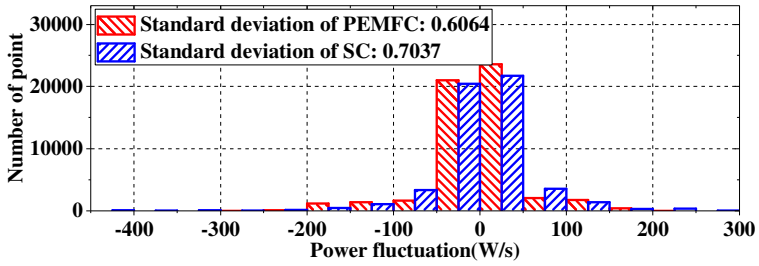

(b)

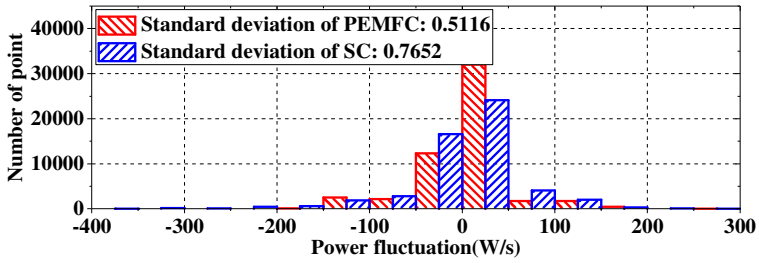

(c)

Fig. 16. Power fluctuation rate distribution of PEMFC and SC using different strategies. (a) SMC strategy; (b) ECMS; (c) OES-EMS.

It can be seen from Fig. 16 that, compared with the SMC strategy and ECMS, the operating stress of PEMFC is the lowest under the control of the presented OES-EMS. Thence, the presented strategy can effectively smooth the fluctuation of PEMFC output power, thereby prolonging the lifetime of PEMFC. Although the operating stress of SC is not the lowest, SC has the advantages of strong durability and long cycle lifespan, so it can be proved that the proposed OES-EMS can improve the system performance.

Furthermore, to highlight the superiority of the presented strategy more clearly, all the results using different strategies are summarized in TABLE VI.

TABLE VI. Performance comparative analysis of different strategies.

	SMC	ECMS	OES-EMS
SOC variation of SC	74.00%-88.92%	74.00%-47.95%	74.00%-72.56%
PEMFC average efficiency	37.12%	32.47%	38.09%
Total hydrogen consumption	32.47g	23.80g	18.21g
PEMFC operating stress	0.8871	0.6064	0.5116

As shown in TABLE VI, among these three strategies, the proposed OES-EMS has advantages in hydrogen consumption, power sources operating stress, efficiency, and SOC of SC.

4.5. Effect verification of constraint D_{FC}

In addition, the comparative analysis of experiments 4 and 5 show the effect of constraint D_{FC} on the experimental results. According to [33] and [38], the longer the operating time of PEMFC under transient load conditions, the more severe the degradation and the shorter the lifetime. Therefore, when the stack is degraded, the stack output power fluctuation should be limited to improve its performance.

Moreover, the results of the power fluctuation distribution of S-1300 No.1 are shown in Fig. 17. It can be seen that compared with the strategy without constraint D_{FC} (D_{FC}=1 during the entire operating cycle), the strategy with constraint D_{FC} is more conducive to limiting PEMFC power dynamics and mitigating the operating stress of PEMFC, thereby extending the lifetime of PEMFC.

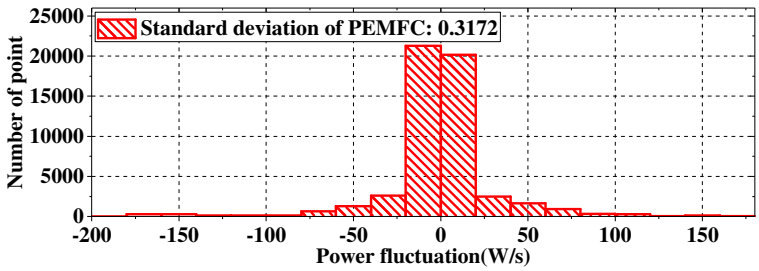

(a)

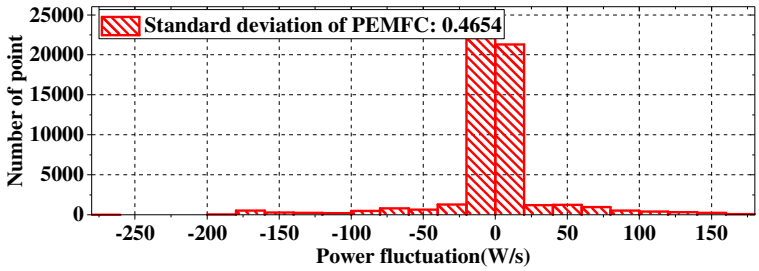

(b)

Fig. 17. PEMFC power fluctuation rate distribution using the proposed OES-EMS. (a) With constraint D_{FC}; (b) Without constraint D_{FC}.

In summary, it could be observed in Fig. 13, the SC SOC variation between the beginning state and end state of OES-EMS is significantly smaller than that of ECMS and SMC strategy. In order to make a clear comparison, the efficiency and hydrogen consumption of the system under the control of different strategies are shown in Figs. 14 and 15. Moreover, the power sources operating stress analysis using different strategies is presented in Fig. 16. At last, to compare and analyze the influence of constraint D_{FC} on experimental results, the PEMFC output power fluctuation distribution is shown in Fig. 17.

5. Conclusion

In this work, an online extremum seeking-based optimized energy management strategy is presented for the fuel cell/supercapacitor hybrid electric tram. Considering that the fuel cell is a complex nonlinear system, an online extremum seeking method is used to estimate the maximum efficiency and maximum power points of the fuel cell. Therefore, the boundary values of the "safe operating zone" can be updated in real-time. The adaptive recursive least square algorithm is proposed to implement this process. According to the structure of the 100% low floor light rail vehicle, a reduced-scale test platform powered by supercapacitor and fuel cell is established, and the scaled-down

driving cycle of the tram is adopted to test the performance of the presented online extremum seeking-based optimized energy management strategy. The results show that, compared with the state machine control strategy and the equivalent consumption minimization strategy, the presented strategy can save 43.92% and 23.49% hydrogen consumption as well as improve the stack efficiency of 2.61% and 17.31%, respectively. In addition, the proposed strategy can also obtain the minimum stack operating stress and minimum SOC variation. This indicates that the presented strategy can ameliorate fuel cell performance, keep the initial state SOC of SC consistent with its final state SOC, save hydrogen consumption, and smooth out the output power fluctuations of fuel cell. Furthermore, the results of this work provide a basis for further research on power allocation between power sources in the 100% low floor light rail vehicle.

Acknowledgements

The authors would like to thank the reviewers for their helpful suggestions. This work was supported by the National Natural Science Foundation (51977181, 52077180) and Fok Ying-Tong Education Foundation of China (171104).

References

[1]. Q. Li, B. Su, Y. Pu, Y. Han, T. Wang, L. Yin, and W. Chen, “A State Machine Control Based on Equivalent Consumption Minimization for Fuel Cell/ Supercapacitor Hybrid Tramway,” *IEEE Transactions on Transportation Electrification*, vol. 5, no. 2, pp. 552–564, Jun. 2019.

[2]. Y. Zhou, A. Ravey, and M.-C. Péra, “Multi-mode predictive energy management for fuel cell hybrid electric vehicles using Markov driving pattern recognizer,” *Applied Energy*, vol. 258, p. 114057, Jan. 2020.

[3]. Y. Yan, Q. Li, W. Chen, B. Su, J. Liu, and L. Ma, "Optimal Energy Management and Control in Multimode Equivalent Energy Consumption of Fuel Cell/Supercapacitor of Hybrid Electric Tram," *IEEE Trans. Ind. Electron.*, vol.66, no.8, pp.6065-6076, Aug. 2019.

[4]. R. Mezzi, N. Yousfi-Steiner, M. C. Péra, D. Hissel, and L. Larger, "An Echo State Network for fuel cell lifetime prediction under a dynamic micro-cogeneration load profile," *Applied Energy*, p. 116297, Dec. 2020.

[5]. Z. Sun, Y. Wang, Z. Chen, and X. Li, "Min-max game based energy management strategy for fuel cell/supercapacitor hybrid electric vehicles," *Applied Energy*, vol. 267, p. 115086, Jun. 2020.

[6]. N. Bizon, "Efficient fuel economy strategies for the Fuel Cell Hybrid Power Systems under variable renewable/load power profile," *Applied Energy*, vol. 251, p. 113400, Oct. 2019.

[7]. Q. Li, W. Yang, L. Yin, and W. Chen, "Real-Time Implementation of Maximum Net Power Strategy Based on Sliding Mode Variable Structure Control for Proton-Exchange Membrane Fuel Cell System," *IEEE Transactions on Transportation Electrification*, vol. 6, no. 1, pp. 288–297, Mar. 2020.

[8]. G. Zhang, Q. Li, W. Chen, and X. Meng, "Synthetic Strategy Combining Speed Self-adjusting Operation Control and Adaptive Power Allocation for Fuel Cell Hybrid Tramway," *IEEE Trans. Ind. Electron.*, pp. 1–1, 2020.

[9]. Y. Yan, Q. Li, W. Huang, and W. Chen, "Operation Optimization and Control Method Based on Optimal Energy and Hydrogen Consumption for the Fuel Cell/Supercapacitor Hybrid Tram," *IEEE Transactions on Industrial Electronics*, vol. 68, no. 2, pp. 1342–1352, Feb. 2021.

[10]. W. Zhang, J. Li, L. Xu, and M. Ouyang, "Optimization for a fuel cell/battery/capacity tram with equivalent consumption minimization strategy," *Energy Convers. & Management*, vol.134, pp.59-69, Dec. 2017.

[11]. T. Wang, Q. Li, X. Wang, Y. Qiu, M. Liu, X. Meng, J. Li, and W. Chen, "An optimized energy management strategy for fuel cell hybrid power system based on maximum efficiency range identification," *J. Power Sources*, vol. 445, p. 227333, Jan. 2020.

[12]. N. Sulaiman, M. A. Hannan, A. Mohamed, P. J. Ker, E. H. Majlan, and W. R. Wan Daud, "Optimization of energy management system for fuel-cell hybrid electric vehicles: Issues and recommendations," *Applied Energy*, vol. 228, pp. 2061–2079, Oct. 2018.

[13]. J. Chen, C. Xu, C. Wu, and W. Xu, "Adaptive fuzzy logic control of fuel-cell-battery hybrid systems for electric vehicles," *IEEE Trans. Ind. Informat.*, vol.14, no.1, pp.292-300, Jan. 2018.

[14]. X. Zhang, C. Mi, A. Masrur, and D. Daniszewski, "Wavelet-transform-based power management of hybrid vehicles with multiple on-board energy sources including fuel cell, battery and ultracapacitor," *J. Power Sources*, vol.185, no.2, pp. 1533-1543, Dec. 2008.

[15]. H. Li, A. Ravey, A. N'Diaye, and A. Djerdir, "Online adaptive equivalent consumption minimization strategy for fuel cell hybrid electric vehicle considering power sources degradation," *Energy Convers. & Management*, vol.192, pp.133-149, Jul. 2019.

[16]. M. Kandidayeni, A. Macias, A. Amamou, L. Boulon, S. Kelouwani, and H. Chaoui, "Overview and benchmark analysis of fuel cell parameters estimation

for energy management purposes," *J. Power Sources*, vol.380, pp.92-104, Mar. 2018.

[17]. K. Ettihir, L. Boulon, and K. Agbossou, "Optimization-based energy management strategy for a fuel cell/battery hybrid power system," *Appl. Energy*, vol.163, pp.142-153, Feb. 2016.

[18]. B. Zhang, J. Zhang, F. Xu, and T. Shen, "Optimal control of power-split hybrid electric powertrains with minimization of energy consumption," *Applied Energy*, vol. 266, p. 114873, May 2020.

[19]. A. M. Ali, A. Ghanbar, and D. Soffker, "Optimal Control of Multi-Source Electric Vehicles in Real Time Using Advisory Dynamic Programming," *IEEE Transactions on Vehicular Technology*, vol. 68, no. 11, pp. 10394–10405, Nov. 2019.

[20]. Q. Li, T. Wang, C. Dai, W. Chen, and L. Ma, "Power management strategy based on adaptive droop control for a fuel cell-battery-supercapacitor hybrid tramway," *IEEE Trans. Veh. Technol.*, vol.67, no.7, pp.5658-5670, Jun. 2017.

[21]. T. Wang, Q. Li, L. Yin, and W. Chen, "Hydrogen consumption minimization method based on the online identification for multi-stack PEMFCs system," *Int. J. Hydrogen Energy*, vol.44, no.11, pp.5074-5081, Feb. 2019.

[22]. S. Kelouwani, K. Adegnon, K. Agbossou, and Y. Dube, "Online system identification and adaptive control for pem fuel cell maximum efficiency tracking," *IEEE Trans. Energy Convers.*, vol. 27, no. 3, pp. 580–592, Sep. 2012.

[23]. J. Wu, X.-Z. Yuan, J. J. Martin, H. Wang, D. Yang, J. Qiao, and J. Ma, "Proton exchange membrane fuel cell degradation under close to open-circuit conditions," *J. Power Sources*, vol. 195, no. 4, pp. 1171–1176, Feb. 2010.

[24]. D. Feroldi, M. Serra, and J. Riera, "Energy Management Strategies based on efficiency map for Fuel Cell Hybrid Vehicles," *J. Power Sources*, vol. 190, no. 2, pp. 387–401, May 2009.

[25]. D. Li, Y. Yu, Q. Jin, and Z. Gao, "Maximum power efficiency operation and generalized predictive control of PEM (proton exchange membrane) fuel cell," *Energy*, vol.68, no.4, pp.210-217, Apr. 2014.

[26]. N. Noura, L. Boulon, and S. Jemei, "An Online Identification Based Energy Management Strategy for a Fuel Cell Hybrid Electric Vehicle," *2019 IEEE Vehicle Power and Propulsion Conference (VPPC)*, Oct. 2019.

[27]. T. Wang, Q. Li, Y. Qiu, L. Yin, L. Liu, and W. Chen, "Efficiency Extreme Point Tracking Strategy Based on FFRLS Online Identification for PEMFC System," *IEEE Trans. Energy Convers.*, vol.34, no.2, pp.952-963, Jun. 2019.

[28]. M. Yue, S. Jemei, R. Gouriveau, and N. Zerhouni, "Review on health-conscious energy management strategies for fuel cell hybrid electric vehicles: Degradation models and strategies," *Int. J. Hydrogen Energy*, vol. 44, no. 13, pp. 6844–6861, Mar. 2019.

[29]. M. Yue, S. Jemei, and N. Zerhouni, "Health-Conscious Energy Management for Fuel Cell Hybrid Electric Vehicles Based on Prognostics-Enabled Decision-Making," *IEEE Trans. Veh. Technol.*, vol. 68, no. 12, pp. 11483–11491, Dec. 2019.

[30]. K. Ettihir, M. Higuita Cano, L. Boulon, and K. Agbossou, "Design of an adaptive EMS for fuel cell vehicles," *Int. J. Hydrogen Energy*, vol. 42, no. 2, pp. 1481–1489, Jan. 2017.

[31]. A. Macias Fernandez, M. Kandidayeni, L. Boulon, and H. Chaoui, "An Adaptive State Machine Based Energy Management Strategy for a Multi-Stack Fuel Cell Hybrid Electric Vehicle," *IEEE Trans. Veh. Technol.*, vol. 69, no. 1, pp. 220–234, Jan. 2020.

[32]. H. Li, A. Ravey, A. N'Diaye, and A. Djerdir, "Equivalent consumption minimization strategy for fuel cell hybrid electric vehicle considering fuel cell degradation," *2017 IEEE Transportation Electrification Conference and Expo* (ITEC), Jun. 2017.

[33]. T. Wang, Q. Li, H. Yang, L. Yin, Y. Qiu, and W. Chen, "Adaptive Current Distribution Method for Parallel-Connected PEMFC Generation System Considering Performance Consistency," *Energy Convers. & Management*, vol.196, no.15, pp.866-877, Sep. 2019.

[34]. D. Zhou, A. Al-Durra, I. Matraji, A. Ravey, and F. Gao, "Online Energy Management Strategy of Fuel Cell Hybrid Electric Vehicles: A Fractional-Order Extremum Seeking Method," *IEEE Trans. Ind. Electron.*, vol. 65, no. 8, pp. 6787–6799, Aug. 2018.

[35]. Y. Yan, Q. Li, W. Chen, W. Huang, and J. Liu, "Hierarchical Management Control Based on Equivalent Fitting Circle and Equivalent Energy Consumption Method for Multiple Fuel Cells Hybrid Power System," *IEEE Trans. Ind. Electron.*, vol. 67, no. 4, pp. 2786–2797, Apr. 2020.

[36]. M. G. Carignano, R. Costa-Castelló, V. Roda, N. M. Nigro, S. Junco, and D. Feroldi, "Energy management strategy for fuel cell-supercapacitor hybrid vehicles based on prediction of energy demand," *J. Power Sources*, vol. 360, pp. 419–433, Aug. 2017.

[37]. J. Chen, D. Zhou, C. Lyu, and C. Lu, "A novel health indicator for PEMFC state of health estimation and remaining useful life prediction," *Int. J. Hydrogen Energy*, vol. 42, no. 31, pp. 20230–20238, Aug. 2017.

[38]. Z. Hua, Z. Zheng, M.-C. Péra, and F. Gao, "Remaining useful life prediction of PEMFC systems based on the multi-input echo state network," *Appl. Energy*, vol. 265, p. 114791, May 2020.

[39]. M. A. Soumeur, B. Gasbaoui, O. Abdelkhalek, J. Ghouili, T. Toumi, and A. Chakar, "Comparative study of energy management strategies for hybrid proton exchange membrane fuel cell four wheel drive electric vehicle," *J. Power Sources*, vol. 462, p. 228167, Jun. 2020.

[40]. Z. Hong, Q. Li, Y. Han, W. Shang, Y. Zhu, and W. Chen, "An energy management strategy based on dynamic power factor for fuel cell/battery hybrid locomotive," *Int. J. Hydrogen Energy*, vol. 43, no. 6, pp. 3261–3272, Feb. 2018.

[41]. L. Xu, J. Li, J. Hua, X. Li, and M. Ouyang, "Adaptive supervisory control strategy of a fuel cell/battery-powered city bus," *J. Power Sources*, vol.194, no.1, pp. 360-368, Oct. 2009.